Earth Syst. Sci. Data Discuss., 6, 1–26, 2013
www.earth-syst-sci-data-discuss.net/6/1/2013/
doi:10.5194/essdd-6-1-2013

Open Access Earth System Science Data Discussions

Mesospheric CO above Troll station, Antarctica observed by a ground based microwave radiometer

C. Straub[1], P. J. Espy[1], R. E. Hibbins[1], and D. A. Newnham[2]

[1]Norwegian University of Science and Technology (NTNU), Trondheim, Norway
[2]British Antarctic Survey, Cambridge, UK

Received: 14 November 2012 – Accepted: 27 December 2012 – Published: 10 January 2013

Correspondence to: C. Straub (corinne.straub@ntnu.no)

Published by Copernicus Publications.

Abstract

This paper presents mesospheric carbon monoxide (CO) data acquired by the ground-based microwave radiometer of the British Antarctic Survey (BAS radiometer) stationed at Troll station in Antarctica (72° S, 2.5° E, 1270 a.m.s.l.). The data set covers the period from February 2008 to January 2010, however, due to very low CO concentrations below approximately 80 km altitude in summer, profiles can only be retrieved during Antarctic winter. CO is measured for approximately 2 h each day and profiles are retrieved approximately every half hour. The retrieved profiles, covering the pressure range from 1 to 0.01 hPa (approximately 48 to 80 km), are compared to measurements from Aura/MLS and SD-WACCM. This intercomparison reveals a low bias of 0.5 to 1 ppmv at 0.1 hPa (approximately 64 km) and 2.5 to 3.5 ppmv at 0.01 hPa (approximately 80 km) of the BAS microwave radiometer compared to both reference datasets. One explanation for this low bias could be the known high bias of MLS which is in the same order of magnitude. The ground based radiometer shows high and significant correlation (coefficients higher than 0.9/0.65 compared to MLS/SD-WACCM) at all altitudes compared with both reference datasets.

doi:10.5285/DE3E2092-406D-47A9-9205-3971A8DFB4A9

1 Introduction

From the stratosphere to the upper mesosphere carbon monoxide (CO) mixing ratios increase by one order of magnitude. The large reservoir of mesospheric and lower thermospheric (75–100 km) CO is mainly produced by ultra-violet photodissociation of carbon dioxide (CO_2). The photochemical loss of CO in the stratosphere and mesosphere is governed primarily by the oxidation reaction with hydroxyl (OH) to form CO_2 (Minschwaner et al., 2010). During the polar night the lifetime of mesospheric CO is longer than 30 days, which, together with its strong vertical gradient in the mesosphere, makes it a valuable tracer for dynamics. The strong descent of air during winter in the polar middle atmosphere transports CO rich air down towards the stratosphere, leading to a downward tilt of the CO isopleth towards the winter pole. In the past, CO measurements have been used to infer rates of polar descent (e.g. Allen et al., 2000; Forkman et al., 2005; Lee et al., 2011) as well as to study horizontal transport during strong dynamical events such as stratospheric sudden warmings (e.g. Manney et al., 2009).

Remote sensing observations of CO in the microwave region using the rotational transitions at 115 GHz and 230 GHz have been performed since 1976 (Waters et al., 1976). Until the early 2000's such measurements have been mostly on a campaign basis focusing on seasonal variations at mid latitudes (e.g. Clancy et al., 1984; Bevilacqua et al., 1985; Aellig et al., 1995). Recently, however, three ground-based radiometers measuring CO have been installed in the Northern Hemisphere at high latitudes and are taking measurements on a regular basis: the radiometer in Onsala, Sweden described in Forkman et al. (2012) from 2002 to 2008 (continuation planned), the radiometer in Kiruna, Sweden described in Hoffmann et al. (2011) since 2008 and the instrument in Thule, Greenland described in Biagio et al. (2010) taking measurements every January to March since 2009.

This paper describes ground-based measurements of mesospheric CO taken from Antarctica. The profiles presented are stored in the database of the British Antarctic Survey.

2 Measurement

The ground-based microwave radiometer of the British Antarctic Survey (BAS) measures spectra in the region of the rotational transitions centered at 250.796 GHz (nitric oxide, NO), 249.79 GHz and 249.96 GHz (ozone, O_3) and 230.538 GHz (carbon monoxide, CO). The instrument has been designed in order to study the effects of energetic particle precipitation on the middle and upper atmosphere, using the NO and O_3 data (e.g. Newnham et al., 2011; Daae et al., 2013). This paper focuses on the

ESSDD
6, 1–26, 2013

CO measurements carried out for approximately 2 h each day in order to study the dynamical context. The data presented have been acquired between February 2008 and January 2010 at Troll station in Antarctica (72° S, 2.5° E, 1270 a.m.s.l.).

2.1 Instrument

The BAS radiometer consists of a highly sensitive, cryogenically cooled radiometer front-end which has been coupled to a spectrometer back-end. It has been designed and manufactured by Radiometer Physics GmbH in Meckenheim, Germany. The radiometer is a robust system for continuous, semi-autonomous operation in the challenging Antarctic environment that requires a minimum of maintenance and operator intervention. The front-end, schematically shown in Fig. 1, comprises a heterodyne receiver where the incoming radiation is combined with one of two independent local oscillators at 255.6 and 225.6 GHz for the NO/O_3 and CO observations, respectively, by a Superconductor-Insulator-Superconductor (SIS) mixer. The intermediate frequency (IF) signal in the 4–6 GHz range is subsequently amplified by an IF amplifier. Each of the signal bands is analyzed using a moderate-resolution as well as a high-resolution chirp transform spectrometer (CTS) (Hartogh, 1998). For the CO measurements the moderate-resolution CTS was used.

The instrument has been described in detail in Espy et al. (2006). However, before the operation presented here there have been two changes to the originally planned set-up: (1) the moderate-resolution CTS has a bandwidth of 220 MHz and a resolution of 29 kHz (not 400 MHz and 100 kHz) and (2) the hot calibration load is at room temperature (approximately 294 K) and the cold load at 60 K (not 60 K and 4 K).

2.2 Calibration and tropospheric correction

A three-way mechanical chopper system selects the microwave signal either from the main reflector pointing to the sky at 30° elevation angle, a 60 K cold load or an ambient-temperature calibration load mounted on the chopper wheel, and directs it into the

Discussion Paper | Discussion Paper | Discussion Paper | Discussion Paper |

ESSDD

6, 1–26, 2013

Mesospheric CO above Troll station, Antarctica

C. Straub et al.

main receiver. The sky signal is then calibrated using the switching technique of Dicke and Beringer (1946) as described by e.g. Parrish (1994) and references therein. Each calibration cycle takes 27 s with 8 s integration time on each target.

For the profile retrieval we correct each calibrated CO emission spectrum for attenuation in the troposphere by mainly water vapor. The factor for the tropospheric correction is calculated as described in Forkman et al. (2012).

2.3 Dataset

The data presented in this paper are from the BAS radiometer's first period of operation in Antarctica between February 2008 and January 2010 at the Norwegian station Troll. In summer, the mesospheric CO mixing ratios fall below the instrument's sensitivity level resulting in negative retrieved volume mixing ratios (VMR) at certain altitudes, and therefore the data recorded during the months March to October only are analyzed. The CO line is observed for approximately two hours each day. As the change from the local oscillator (LO) used for NO and O_3 measurements to the LO for the CO measurements was done manually by an operator, the measurement times vary slightly, e.g. 80 % of the data are recorded between ±2 h of local noon, and there are a 98 days without CO measurements. In order to achieve a high enough signal to noise ratio for the profile retrieval, several measured spectra are integrated. For this study 80 spectra from consecutive calibration cycles are averaged, which under good observing conditions results in a measurement noise of less than 0.15 K and an integration time of less than 30 min. Spectra with measurement noise higher than 0.25 K, due to e.g. high tropospheric opacity, are not considered for profile retrieval. During the winters 2008 and 2009 (492 measurement days) the radiometer acquired a total of 1974 integrated spectra over 394 days that are suited for profile retrieval.

A typical integrated spectrum (average of 80 spectra, integration time approximately 24 min) is shown in Fig. 2. A large baseline resulting from standing waves in the front-end is visible. However, when just focusing on an area of 40 MHz around the CO

ESSDD
6, 1–26, 2013

line-center, indicated by the black solid lines, the baseline can be approximated by a 6th order polynomial curve fitted to the data.

From February 2008 to the beginning of August the shape of the measured CO spectra was similar to the one shown in the top panel of Fig. 3. However, on 9 August 2008 a sudden change occurred, and the spectrum acquired shoulders located approximately ±1 MHz on either side of the CO line center (compare lower panel of Fig. 3). The reason for this feature was found to be an instability in the electronic phase-lock control of the 225.6 GHz local oscillator. For the profile retrieval such a feature, being symmetrical around the line center, poses a significant limitation. However, as the feature was stable in amplitude and position over time, we applied an empirical correction to the channel response function of the spectrometer during the retrieval process (description in Sect. 3.1). This allowed realistic CO profiles to be retrieved even after the feature appeared.

3 Retrieval of vertical profiles

The inversions of the CO spectra are performed using the optimal estimation method (Rodgers, 2000) implemented in the Qpack software package (v2.0.0) (Eriksson et al., 2005). The forward model is provided by the Atmospheric Raditative Transfer Simulator (ARTS), a modular program simulating atmospheric radiative transfer (Eriksson et al., 2011). For a detailed description of the retrieval of CO profiles using ARTS and QPack we refer the reader to Hoffmann et al. (2011) and Forkman et al. (2012). Here we will focus on the discussion of the retrieval setup and the results, including error estimates, of the measurements in Antarctica.

ESSDD
6, 1–26, 2013

Title Page
Abstract | Instruments
Data Provenance & Structure
Tables | Figures
◂◂ | ▸▸
◂ | ▸
Back | Close
Full Screen / Esc
Printer-friendly Version
Interactive Discussion

3.1 Retrieval set-up

For the inversions the measured spectrum is limited to 40 MHz centered on the CO line at 230.538 GHz. The retrieved quantities are CO volume mixing ratio, instrumental baseline in the form of a polynomial of 6th degree and a frequency offset.

The line parameters, as input for the forward model, are taken from the HITRAN 2004 spectroscopic database Rothman et al. (2005). The apriori temperature and CO profiles are constructed from NCAR's Whole Atmosphere Community Climate Model with Specified Dynamics (SD-WACCM) data (Lamarque et al., 2012) (description in Sect. 4.2). A monthly mean 20 yr climatology is used for the center date of each month, and the values for the days in between are found by linear interpolation. The CO apriori covariance is held constant at 10 % of the mean apriori profile throughout the year. This value is comparable to the daily standard deviation of 20 yr of SD-WACCM data in the altitude range we expect the BAS radiometer to be sensitive, and somewhat smaller at higher altitudes (above 0.01 hPa, 80 km). In addition to the diagonal elements, the shape of the apriori covariance matrix is defined as linearly decreasing toward the off-diagonal elements with a correlation length of a quarter of a pressure decade (approximately 4 km).

Before 9 August 2008 the channel response function of the spectrometer is approximated with the sinc function (full width at half maximum of 50 kHz) shown in Fig. 4. After that date an empirical correction in the form of two secondary sinc functions centered at approximately ±1 MHz from the center frequency is applied to the channel response function (also shown in Fig. 4) in order to correct for the feature caused by the local oscillator.

3.2 Results of the measurements

The results of two typical measurement of the radiometer are shown in Fig. 5 (top panel before and bottom panel after 9 August 2008). The measured and fitted spectrum, and the difference between the two (residuals) shown in the left panels, indicate that the

ESSDD
6, 1–26, 2013

measured spectrum is fitted accurately and the residuals contain mainly noise contributions (standard deviation of the residuals $\sigma = 0.18$ and 0.14 for the 2008 and 2009 spectrum, respectively).

The middle panels indicate that the retrieval has enough freedom in order to estimate a profile clearly different from the apriori even though the apriori covariance used in the inversion is small. The right panels show the Averaging Kernels (AVK) of the inversion, which describe the relationship between the true, apriori and retrieved state of the atmosphere. None of the AVK, even those at higher altitudes, peak above 0.05 hPa (approximately 68 km), which is the altitude where Doppler broadening starts to dominate over pressure broadening. This indicates that at this pressure level and above the retrieval does not provide any altitude profile information, even though it is still sensitive to variations in the CO VMR. The area of the AVK, also shown in the right panels of Fig. 5, indicates that the retrieved profile is determined by the true atmospheric state at altitudes between approximately 1 and 0.01 hPa (area of the AVK > 0.8).

The degree of freedom (trace of the AVK matrix) is approximately 2 indicating that 2 independent layers are retrieved in the valid altitude range. This means that the vertical resolution of the retrieval is approximately 15 km.

3.3 Error characterization

The estimation of the 1-σ random measurement error on the radiometer's profiles is based on Rodgers (2000), meaning that the measurement noise on the spectra is propagated through the inversion. The 2-σ systematic errors are estimated by perturbing the retrieval set-up with the uncertainties of the temperature profile as well as the calibration and the intensity of the CO line. The temperature profile was perturbed with 5 K (1-σ of 20 yr of monthly SD-WACCM data is between 2.5 and 4 K at all altitudes) and the intensity of the CO line with 2 %, following the suggestion of Hoffmann et al. (2011). The uncertainty in the radiometer calibration is estimated to have an upper limit of 10 % of the tropospheric correction factor. This estimate accounts for uncertainties in the temperatures of the calibration loads, the observation angle and standing waves

ESSDD
6, 1–26, 2013
Mesospheric CO above Troll station, Antarctica
C. Straub et al.

on the spectra, as well as for uncertainties in the factor for the tropospheric correction itself.

In addition, we give an upper limit for the systematic error induced by the empirical correction to the channel response function after 9 August 2008. We estimate this error by differencing the profiles inverted with a sinc function with FWHM of 50 kHz (blue in Fig. 4) with those made using the modified sinc function (red in Fig. 4).

The results of the error calculations are displayed in Fig. 6. The plot indicates that the uncertainty induced by the modified channel response function after 9 August 2008 dominates the systematic error and therefore we conclude that the shape of the channel response function is a critical parameter for the absolute values of the retrieved profile. In laboratory experiments the channel response of the CTS was characterized 0.5 MHz about the linecenter. However, this frequency range proved to not be sufficient for the backend characterization in the profile retrieval and therefore a sinc function was used as an approximation. This might introduce an additional systematic error which we have not been able to characterize here.

4 Comparison to Aura/MLS and SD-WACCM

In this section we present a comparison between the CO VMRs retrieved from the measurements of the BAS radiometer, the values found by the Microwave Limb Sounder on the Aura satellite (Aura/MLS) and modeled values from the Whole Atmosphere Community Climate Model with Specified Dynamics (SD-WACCM). The three different timeseries on two pressure levels in the mesosphere (0.3 and 0.03 hPa, approximately 56 and 72 km) are shown in Fig. 7 indicating good general agreement. For these plots (described below) the values closest to the indicated pressure levels are used without taking differences in the vertical resolution of the datasets into account.

ESSDD
6, 1–26, 2013
Mesospheric CO above Troll station, Antarctica
C. Straub et al.

4.1 Aura/MLS

The Aura satellite is in a Sun-synchronous orbit passing through two local times at latitudes up to 82.5°. The MLS instrument is described in Waters et al. (2006); a validation of the CO measurements (version 2.2) is given in Pumphrey et al. (2007); and an overview of the version 3.3 retrievals is given in Livesey et al. (2011). We use the MLS version 3.3 CO product which covers the pressure range 215 to 0.005 hPa with a vertical resolution of approximately 6 km throughout the mesosphere. The single profile precision (1-σ random error estimated from the level 2 algorithms) degrades throughout the mesosphere from 0.15 ppmv at 1 hPa to 4 ppmv at 0.01 hPa, and the validation against ACE/FTS suggests that MLS has a positive bias between 30 and 50 % throughout the mesosphere (Waters et al., 2006; Livesey et al., 2011).

For the intercomparison we use MLS profiles within a range of ±1° in latitude and ±5° in longitude from Troll station.

4.2 SD-WACCM

WACCM is a comprehensive chemistry-climate model using a free-running dynamical core that is adopted from the NCAR Community Atmosphere Model (CAM). Its chemistry module is an extension of version 3 of the Model of OZone And Related Tracers (MOZART3), e.g. Kinnison et al. (2007). The gravity wave parameterization in WACCM (Richter et al., 2010) simulates effects of unresolved gravity wave sources such as topography, convection (mostly in low latitudes), and frontal dynamics (middle and high latitudes). The parameterization also gives a coefficient for vertical eddy diffusion that affects heating and the mixing ratios of trace species. For the specified dynamics (SD) runs described in Lamarque et al. (2012), wind and temperature fields are nudged at each model time step using the Goddard Earth Observing System 5 (GEOS-5) analysis. The specified dynamics option allows to use WACCM as a chemical transport model which facilitates the comparisons with observations of trace chemical species as the state of the real atmosphere at a given time is reproduced. The SD-WACCM run

Discussion Paper | Discussion Paper | Discussion Paper | Discussion Paper |
ESSDD
6, 1–26, 2013
Mesospheric CO above Troll station, Antarctica
C. Straub et al.
Title Page
Abstract Instruments
Data Provenance & Structure
Tables Figures
◂◂ ▸▸
◂ ▸
Back Close
Full Screen / Esc
Printer-friendly Version
Interactive Discussion

used for this intercomparison is nudged with 1 % of the GEOS-5 meteorological fields below 60 km (e.g. temperature, zonal and meridional winds, and surface pressure) every 30 min. Latitude and longitude resolution for these WACCM runs is $1.9^\circ \times 2.5^\circ$ and there are 88 pressure levels from the surface to 150 km altitude. For the intercomparison we use the WACCM midnight profile at the grid point (72.95° S, 2.5° E) closest to Troll station.

4.3 Coincident data

A set of coincident profiles is generated by first searching for all the profiles from the BAS radiometer within one day. Then we take the mean of the time of all profiles found on a certain day, and search for all MLS (WACCM) profiles within 12 h before and after that time. From this set of profiles we use the MLS (WACCM) and BAS radiometer profile closest in time. This strategy results in 312 (394) coincident profiles that are not interdependent. We henceforth refer to the coincident profiles of MLS and WACCM as the reference profiles.

As MLS and WACCM both have a better altitude resolution than the radiometer the reference profiles are convolved with the AVKs from the radiometer data inversion.

4.4 Results and discussion

The intercomparison strategy used closely follows Stiller et al. (2012) and Tschanz et al. (2012); the results are displayed in Figs. 8 and 9.

The plots to the left of Fig. 8 show the mean coincident profile for each of the three datasets, before 9 August 2008 in the top panel and after in the bottom panel. The comparison indicates that the CO VMRs from the BAS radiometer have a low bias at all altitudes compared to the two reference profiles, while the reference profiles are in good agreement.

The middle panel displays the bias and standard error of the datasets together with the estimated systematic error of the BAS radiometer. The systematic error on the

Discussion Paper | Discussion Paper | Discussion Paper | Discussion Paper |
ESSDD
6, 1–26, 2013
Mesospheric CO above Troll station, Antarctica
C. Straub et al.
Title Page
Abstract Instruments
Data Provenance & Structure
Tables Figures
◀◀ ▶▶
◀ ▶
Back Close
Full Screen / Esc
Printer-friendly Version
Interactive Discussion

reference profiles is assumed to be negligible. The top plot indicates that before 9 August 2008 the low bias of the BAS radiometer is larger than the estimated systematic error at altitudes above 0.05 hPa compared to MLS and at all altitudes compared to SD-WACCM. The bottom plot indicates that after 9 August 2008 this situation has not significantly changed. One explanation for the low bias of the BAS radiometer could be that we underestimate the systematic error of the instrument due to the channel response function not being well characterized. However, when making comparisons with MLS CO data we need to keep in mind that MLS CO profiles have a known high bias of 30–50 % compared to ACE-FTS (Waters et al., 2006; Livesey et al., 2011) (corresponding to approximately 2–3 ppmv at 0.01 hPa and 0.3–0.5 ppmv at 0.1 hPa) in the mesosphere, which could be the explanation for the apparent low bias of the BAS radiometer. Unfortunately the BAS radiometer data can not be directly compare to ACE-FTS due to a lack of coincident profiles. The SD-WACCM profiles have previously been found to be in good agreement with MLS by Hoffmann et al. (2012).

The right panel of Fig. 8 displays the standard deviation of the difference between the profiles together with the combined random errors of the BAS radiometer and MLS. The estimated random error is larger than the standard deviation of the difference hinting towards an overestimation of the random error. The combined estimated uncertainty mainly represents MLS, as the satellite's estimated random error is clearly larger than that of the BAS radiometer. There are no uncertainties provided along with the SD-WACCM profiles.

The correlation coefficients between the timeseries of radiometer profiles and of convolved reference profiles (MLS in the left panel and SD-WACCM in the right panel) at each pressure level are shown in Fig. 9. Separate correlation coefficients have been calculated before and after 9 August 2008. All correlation coefficients displayed are statistically significant to greater than the 5-sigma level.

The correlation between the timeseries of BAS radiometer and MLS CO data is very high, with correlation coefficients higher than 0.9 at all pressure levels and for both time intervals. This indicates that both instruments observe a similar time evolution

Discussion Paper | Discussion Paper | Discussion Paper | Discussion Paper |

ESSDD
6, 1–26, 2013

in mesospheric CO. The correlation coefficients between the BAS radiometer and SD-WACCM are somewhat lower but still statistically significant to greater than the 5-sigma level.

5 Conclusions and outlook

This paper presents mesospheric CO measurements between February 2008 and January 2010 acquired by a ground based microwave radiometer stationed at Troll station, Antarctica. The instrument, measuring CO for approximately 2 h per day, acquired 1974 spectra on 394 days (out of 492 possible days) during the Antarctic winter months of March–October of 2008 and 2009. Under good observing conditions we retrieve a profile covering the pressure range 1 to 0.01 hPa every 30 min.

The retrieved profiles have been compared to measurements of Aura/MLS and model runs of SD-WACCM. This intercomparison indicates a low bias of 0.5 to 1 ppmv at 0.1 hPa and 2.5 to 3.5 ppmv at 0.01 hPa of the BAS radiometer compared to both reference datasets. MLS has a known high bias of the same order of magnitude in the mesosphere which could be the explanation for that intercomparison result. The high and significant correlation of the timeseries at all altitudes indicates that the BAS radiometer monitors realistic short and long term variations of mesospheric CO.

After an upgrade to allow for fully automated switching between NO/O_3 and CO the BAS radiometer will be taken back to Antarctica during the austral summer of 2012/2013 in order to continue measurements of the polar middle atmosphere.

Acknowledgements. We thank Anne K. Smith for providing the SD-WACCM data used in this paper and Patrick Erikson and Ole Martin Christensen for helpfull discussions on the data retrieval. In addition, we thank Mark Clilverd at BAS, Kim Holmen at the Norwegian Polar Institute (NPI) and Paul Hartogh at Max Planck Institute (MPI, Germany) for their support of the BAS microwave radiometer. We also thank the Troll station over-wintering engineers Atle Markussen, Asbjorn Djupdal, and Tore Dahl as well as David Maxfield and Paul Breen at BAS for their help. The work at NTNU has been funded by the Norwegian Polar Institute Antarctic Program under

ESSDD
6, 1–26, 2013

the grant "Observations of carbon monoxide and ozone in the Antarctic and Arctic: Implications for the Inter-hemispheric coupling of vertical motions". The BAS microwave radiometer project is funded in part by the Natural Environment Research Council (UK).

References

Aellig, C. P., Kämpfer, N., and Hauchecorne, A.: Variability of mesospheric CO in the fall and winter as observed with ground-based microwave radiometry at 115 GHz, J. Geophys. Res., 100, 14125–14130, 1995. 3

Allen, D. R., Stanford, J. L., Nakamura, N., López-Valverde, M. A., López-Puertas, M., Taylor, F. W., and Remedios, J. J.: Antarctic polar descent and planetary wave activity observed in ISAMS CO from April to July 1992, Geophys. Res. Lett., 27, 665–668, doi:10.1029/1999GL010888, 2000. 3

Bevilacqua, R. M., Stark, A. A., and Schwartz, P. R.: The Variability of Carbon Monoxide in the Terrestrial Mesosphere as Determined From Ground-Based Observations of the $J = 1 \rightarrow 0$ Emission Line, J. Geophys. Res., 90, 5777–5782, 1985. 3

Biagio, C. D., Muscari, G., di Sarra, A., de Zafra, R. L., Eriksen, P., Fiocco, G., Fiorucci, I., and Fuà, D.: Evolution of temperature, O_3, CO, and N_2O profiles during the exceptional 2009 Arctic major stratospheric warming observed by lidar and mm-wave spectroscopy at Thule (76.5° N, 68.8° W), Greenland, J. Geophys. Res., 115, D24315, doi:10.1029/2010JD014070, 2010. 3

Clancy, R. T., Muhleman, D. O., and Allen, M.: Seasonal Variability of CO in the Terrestrial Mesosphere, J. Geophys. Res., 89, 9673–9676,, 1984. 3

Daae, M., Espy, P. J., Tyssoy, H. N. N., Newnham, D. A., Stadsnes, J., and Soraas, F.: The effect of energetic electron precipitation on middle mesospheric night-time ozone during and after a moderate geomagnetic storm, Geophys. Res. Lett., 39, L21811, doi:10.1029/2012GL053787, 2013. 3

Dicke, R. . H. and Beringer, R.: Microwave radiation from the sun and moon, Astrophys. J., 103, 375–376, 1946. 5

Eriksson, P., Jiménez, C., and Buehler, S. A.: Qpack, a general tool for instrument simulation and retrieval work, J. Q. Spectrosc. Ra., 91, 47–64, 2005. 6

ESSDD
6, 1–26, 2013

Mesospheric CO above Troll station, Antarctica

C. Straub et al.

Eriksson, P., Buehler, S. A., Davis, C. P., Emde, C., and Lemke, O.: ARTS, the atmospheric radiative transfer simulator, version 2, J. Quant. Spectrosc. Ra., 112, 1551–1558, 2011. 6
Espy, P., Hartogh, P., and Holmén, K.: A microwave radiometer for the remote sensing of nitric oxide and ozone in the middle atmosphere, Proceedings of SPIE, 6362, 63620P, doi:10.1117/12.688953, 2006. 4
Forkman, P., Eriksson, P., Murtagh, D., and Espy, P.: Observing the vertical branch of the mesospheric circulation at latitude 60° N using ground-based measurements of CO and H_2O, J. Geophys. Res., 110, D05107, doi:10.1029/2004JD004916, 2005. 3
Forkman, P., Christensen, O. M., Eriksson, P., Urban, J., and Funke, B.: Six years of mesospheric CO estimated from ground-based frequency-switched microwave radiometry at 57° N compared with satellite instruments, Atmos. Meas. Tech., 5, 2827–2841, doi:10.5194/amt-5-2827-2012, 2012. 3, 5, 6
Hartogh, P.: High resolution chirp transform spectrometer for middle atmospheric microwave sounding, in: Satellite Remote Sensing of Clouds and the Atmosphere II, vol. 3220, 115–124, Society of Photographic Instrumentation Engineers, 1998. 4
Hoffmann, C. G., Raffalski, U., Palm, M., Funke, B., Golchert, S. H. W., Hochschild, G., and Notholt, J.: Observation of strato-mesospheric CO above Kiruna with ground-based microwave radiometry – retrieval and satellite comparison, Atmos. Meas. Tech., 4, 2389–2408, doi:10.5194/amt-4-2389-2011, 2011. 3, 6, 8
Hoffmann, C. G., Kinnison, D. E., Garcia, R. R., Palm, M., Notholt, J., Raffalski, U., and Hochschild, G.: CO at 40–80 km above Kiruna observed by the ground-based microwave radiometer KIMRA and simulated by the Whole Atmosphere Community Climate Model, Atmos. Chem. Phys., 12, 3261–3271, doi:10.5194/acp-12-3261-2012, 2012. 12
Kinnison, D. E., Brasseur, G. P., Walters, S., Garcia, R. R., Marsh, D. R., Sassi, F., Harvey, V. L., Randall, C. E., Emmons, L., Lamarque, J. F., Hess, P., Orlando, J. J., Tie, X. X., Randel, W., Pan, L. L., Gettelman, A., Granier, C., Diehl, T., Niemeier, U., and Simmons, A. J.: Sensitivity of chemical tracers to meteorological parameters in the MOZART-3 chemical transport model, J. Geophys. Res., 112, D20302, doi:10.1029/2006JD007879, 2007. 10
Lamarque, J.-F., Emmons, L. K., Hess, P. G., Kinnison, D. E., Tilmes, S., Vitt, F., Heald, C. L., Holland, E. A., Lauritzen, P. H., Neu, J., Orlando, J. J., Rasch, P. J., and Tyndall, G. K.: CAM-chem: description and evaluation of interactive atmospheric chemistry in the Community Earth System Model, Geosci. Model Dev., 5, 369–411, doi:10.5194/gmd-5-369-2012, 2012. 7, 10

ESSDD
6, 1–26, 2013
Mesospheric CO above Troll station, Antarctica
C. Straub et al.

Lee, J. N., Wu, D. L., Manney, G. L., Schwartz, M. J., Lambert, A., Livesey, N. J., Minschwaner, K. R., Pumphrey, H. C., and Read, W. G.: Aura Microwave Limb Sounder observations of the polar middle atmosphere: Dynamics and transport of CO and H_2O, J. Geophys. Res., 116, D05110, doi:10.1029/2010JD014608, 2011. 3

Livesey, N. J., Read, W. G., Froidevaux, L., Lambert, A., Manney, G. L., Pumphrey, H. C., Santee, M. L., Schwartz, M. J., Wang, S., Cofeld, R. E., Cuddy, D. T., Fuller, R. A., Jarnot, R. F., Jiang, J. H., Knosp, B. W., Stek, P. C., Wagner, P. A., and Wu, D. L.: EOS/MLS – Version 3.3 Level 2 data quality and description document, Tech. rep., Jet Propulsion Laboratory, 2011. 10, 12

Manney, G. L., Harwood, R. S., MacKenzie, I. A., Minschwaner, K., Allen, D. R., Santee, M. L., Walker, K. A., Hegglin, M. I., Lambert, A., Pumphrey, H. C., Bernath, P. F., Boone, C. D., Schwartz, M. J., Livesey, N. J., Daffer, W. H., and Fuller, R. A.: Satellite observations and modeling of transport in the upper troposphere through the lower mesosphere during the 2006 major stratospheric sudden warming, Atmos. Chem. Phys., 9, 4775–4795, doi:10.5194/acp-9-4775-2009, 2009. 3

Minschwaner, K., Manney, G. L., Livesey, N. J., Pumphrey, H. C., Pickett, H. M., Froidevaux, L., Lambert, A., Schwartz, M. J., Bernath, P. F., and Walker, K. A.: The photochemistry of carbon monoxide in the stratosphere and mesosphere evaluated from observations by the Microwave Limb Sounder on the Aura satellite, J. Geophys. Res., 115, D13303, doi:10.1029/2009JD012654, 2010. 2

Newnham, D. A., Espy, P. J., Clilverd, M. A., Rodger, C. J., Seppälä, A., Maxfield, D. J., Hartogh, P., Holmén, K., and Horne, R. B.: Direct observations of nitric oxide produced by energetic electron precipitation into the Antarctic middle atmosphere, Geophys. Res. Lett., 38, L20104, doi:10.1029/2011GL048666, 2011. 3

Parrish, A.: Millimeter-wave remote sensing of ozone and trace constituents in the stratosphere, Proc. IEEE, 82, 1915–1929, 1994. 5

Pumphrey, H. C., Filipiak, M. J., Livesey, N. J., Schwartz, M. J., Boone, C., Walker, K. A., Bernath, P., Ricaud, P., Barret, B., Clerbaux, C., Jarnot, R. F., Manney, G. L., and Waters, J. W.: Validation of middle-atmosphere carbon monoxide retrievals from MLS on Aura, J. Geophys. Res., 112, D24S38, doi:10.1029/2007JD008723, 2007. 10

Richter, J. H., Sassi, F., and Garcia, R. R.: Toward a Physically Based Gravity Wave Source Parameterization in a General Circulation Model, J. Atmos. Sci., 67, 136–156, doi:10.1175/2009JAS3112.1, 2010. 10

Rodgers, C. D.: Inverse Methodes for Atmospheric Soundings, World Scientific Publishing Co. Pte. Ltd, Singapore, 2000. 6, 8

Rothman, L. S., Jacquemart, D., Barbe, A., Benner, D. C., Birk, M., Brown, L. R., Carleer, M. R., Chackerian, C., Chance, K., Coudert, L. H., Dana, V., Devi, V. M., Flaud, J.-M., Gamache, R. R., Goldman, A., Hartmann, J.-M., Jucks, K. W., Maki, A. G., Mandin, J.-Y., Massie, S. T., Orphal, J., Perrin, A., Rinsland, C. P., Smith, M. A. H., Tennyson, J., Tolchenov, R. N., Toth, R. A., Auwera, J. V., Varanasi, P., and Wagner, G.: The HITRAN 2004 molecular spectroscopic database, J. Quant. Spectrosc. Ra., 96, 139–204, 2005. 7

Stiller, G. P., Kiefer, M., Eckert, E., von Clarmann, T., Kellmann, S., García-Comas, M., Funke, B., Leblanc, T., Fetzer, E., Froidevaux, L., Gomez, M., Hall, E., Hurst, D., Jordan, A., Kämpfer, N., Lambert, A., McDermid, I. S., McGee, T., Miloshevich, L., Nedoluha, G., Read, W., Schneider, M., Schwartz, M., Straub, C., Toon, G., Twigg, L. W., Walker, K., and Whiteman, D. N.: Validation of MIPAS IMK/IAA temperature, water vapor, and ozone profiles with MOHAVE-2009 campaign measurements, Atmos. Meas. Tech., 5, 289–320, doi:10.5194/amt-5-289-2012, 2012. 11

Tschanz, B., Straub, C., Walker, K., Stiller, G., and Kämpfer, N.: Validation of middle atmospheric water vapor profiles measured by the ground based microwave radiometer MIAWARA-C, in preparation, Atmos. Meas. Tech. Discuss., 2012. 11

Waters, J., Froidevaux, L., Harwood, R., Jarno, R., Pickett, H., Read, W., Siegel, P., Cofield, R., Filipiak, M., Flower, D., Holden, J., Lau, G., Livesey, N., Manney, G., Pumphrey, H., Santee, M., Wu, D., Cuddy, D., Lay, R., Loo, M., Perun, V., Schwartz, M., Stek, P., Thurstans, R., Boyles, M., Chandra, S., Chavez, M., Chen, G.-S., Chudasama, B., Dodge, R., Fuller, R., Girard, M., Jiang, J., Jiang, Y., Knosp, B., LaBelle, R., Lam, J., Lee, K., Miller, D., Oswald, J., Patel, N., Pukala, D., Quintero, O., Scaff, D., Snyder, W., Tope, M., Wagner, P., and Walch, M.: The Earth Observing System Microwave Limb Sounder (EOS MLS) on the Aura satellite, IEEE T. Geosci. Remote Sens., 44, 1075–1092, 2006. 10, 12

Waters, J. W., Wilson, W. J., and Shimabokuro, F. I.: Microwave Measurement of Mesospheric Carbon Monoxide, Science, 191, 1174–1175, 1976. 3

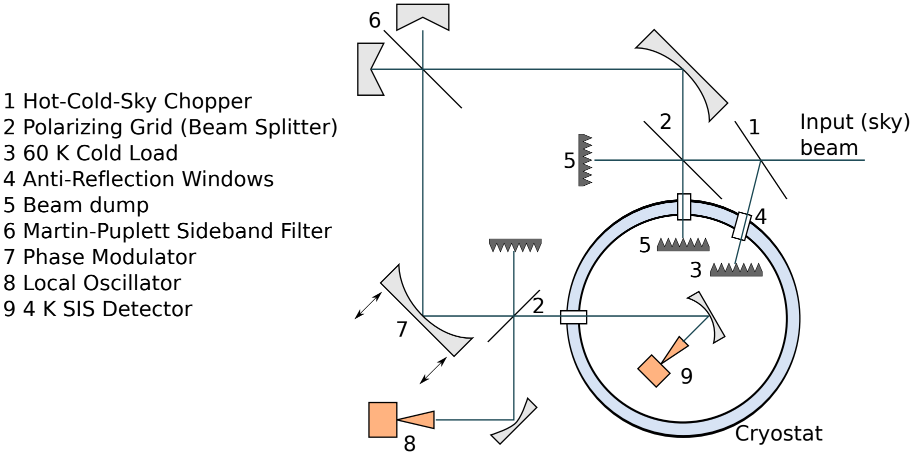

Fig. 1. Schematic drawing of the heterodyne receiver of the BAS microwave radiometer.

ESSDD
6, 1–26, 2013

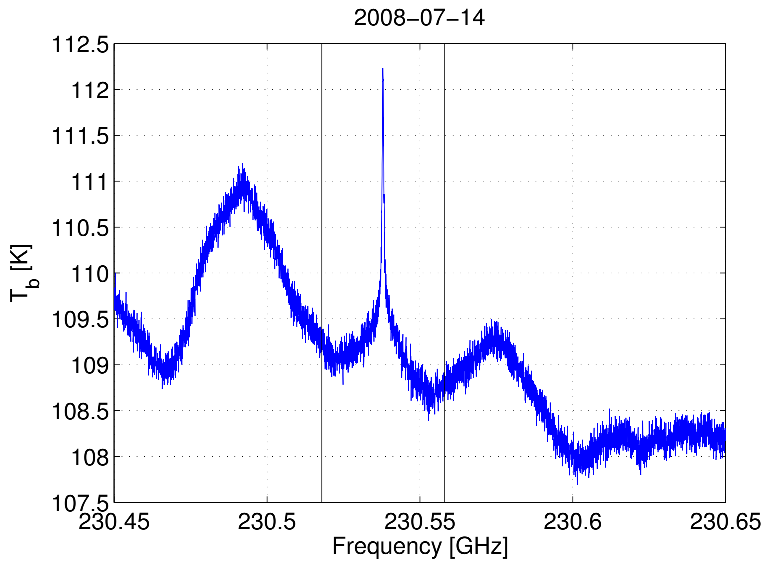

Fig. 2. Calibrated spectrum before tropospheric correction. The solid black vertical lines mark the part of the spectrum used for the profile retrieval.

ESSDD
6, 1–26, 2013

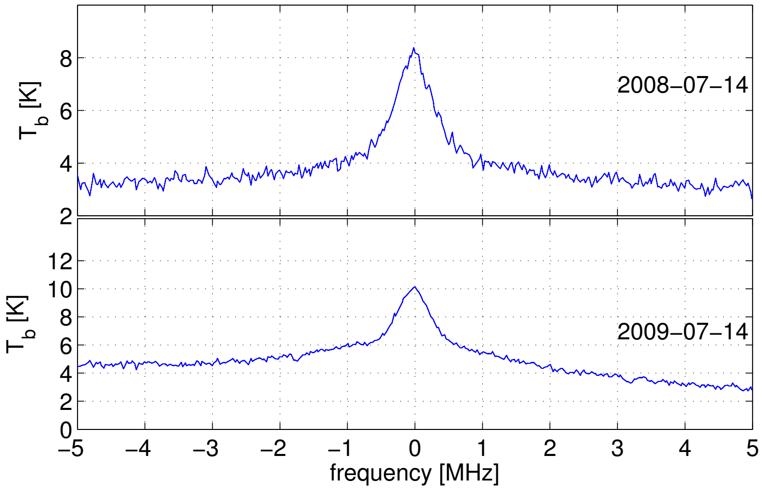

Fig. 3. Calibrated CO spectrum after tropospheric correction as measured before and after 9 August 2008.

ESSDD
6, 1–26, 2013

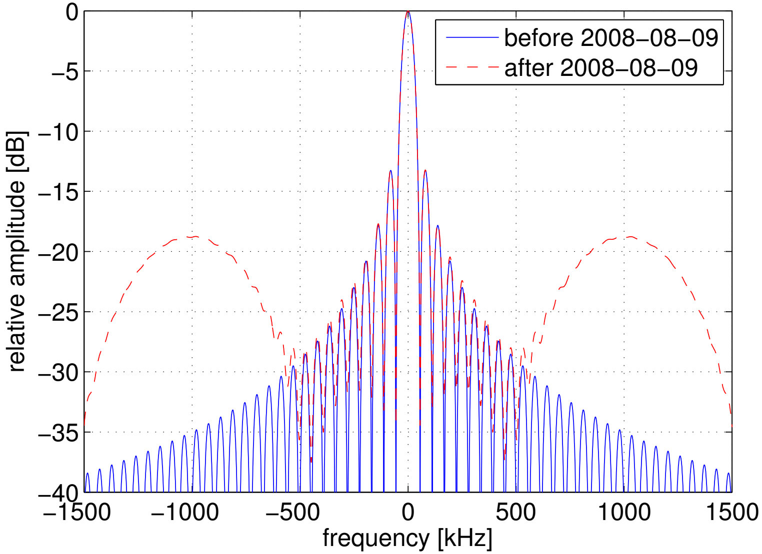

Fig. 4. Channel response functions used in the retrieval before and after 9 August 2008.

ESSDD
6, 1–26, 2013

Mesospheric CO above Troll station, Antarctica

C. Straub et al.

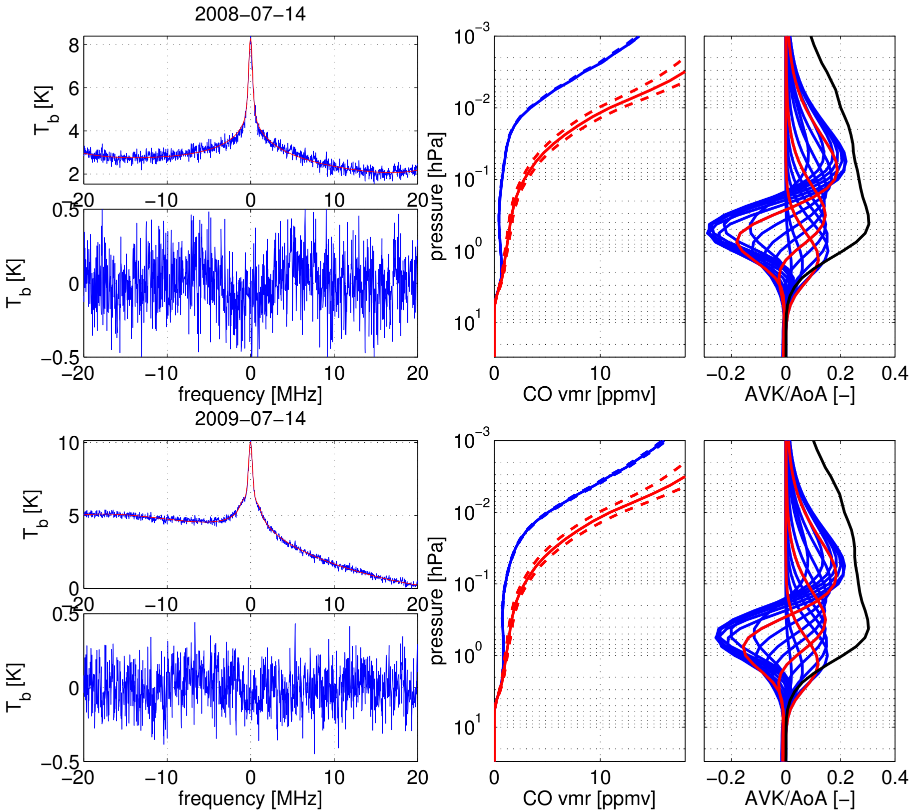

Fig. 5. Retrieval before (top) and after (bottom) 9 August 2008. Left top: calibrated spectrum after tropospheric correction (blue) and fit found using optimal estimation (red). Bottom left: residuals. Middle: estimated atmospheric profile with measurement error (blue) and apriori with covariance (red). Right: AVK (red – 1, 0.1 and 0.01 hPa) and area of the AVK divided by 4 (measurement response).

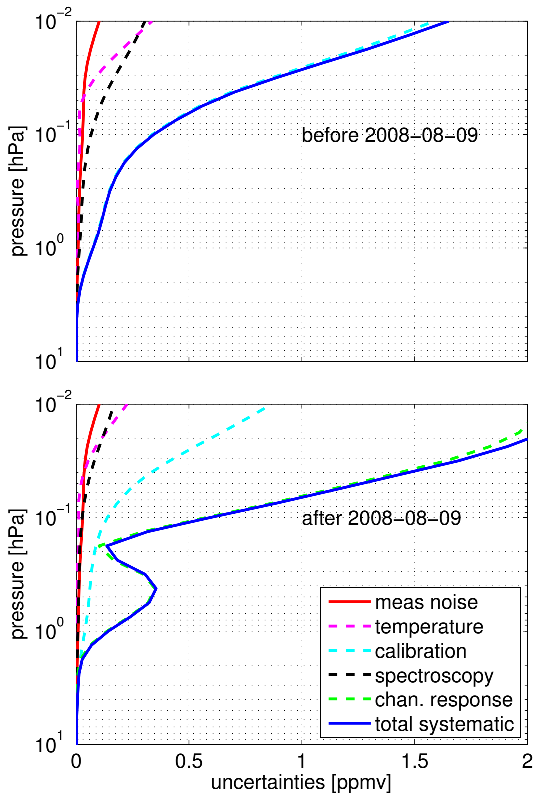

Fig. 6. Estimated uncertainties for the BAS radiometer. The uncertainty caused by the measurement noise (1-σ, red) is regarded as random while the systematic error (2-σ) is determined by perturbing the temperature profile (magenta dashed), calibration (cyan dashed), spectroscopic parameters (blue dashed) and the channel response function (green dashed) with the respective uncertainties. Top: before 9 August 2008, Bottom: after 9 August 2008.

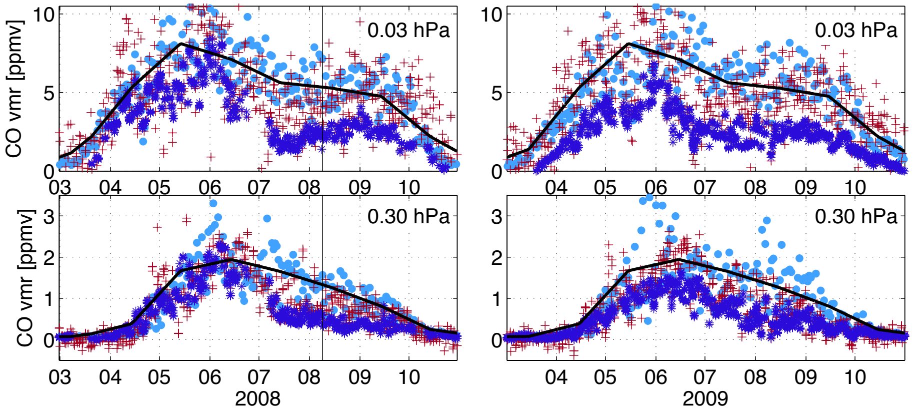

Fig. 7. Time series of the BAS radiometer data (blue $*$) at two pressure levels (top: 0.03 hPa, bottom: 0.3 hPa) for the Antarctic winters 2008 and 2009 together with MLS (red +) and SD-WACCM data above Troll station (light blue •). The black line indicates the apriori VMR used in the BAS radiometers retrieval.

ESSDD
6, 1–26, 2013

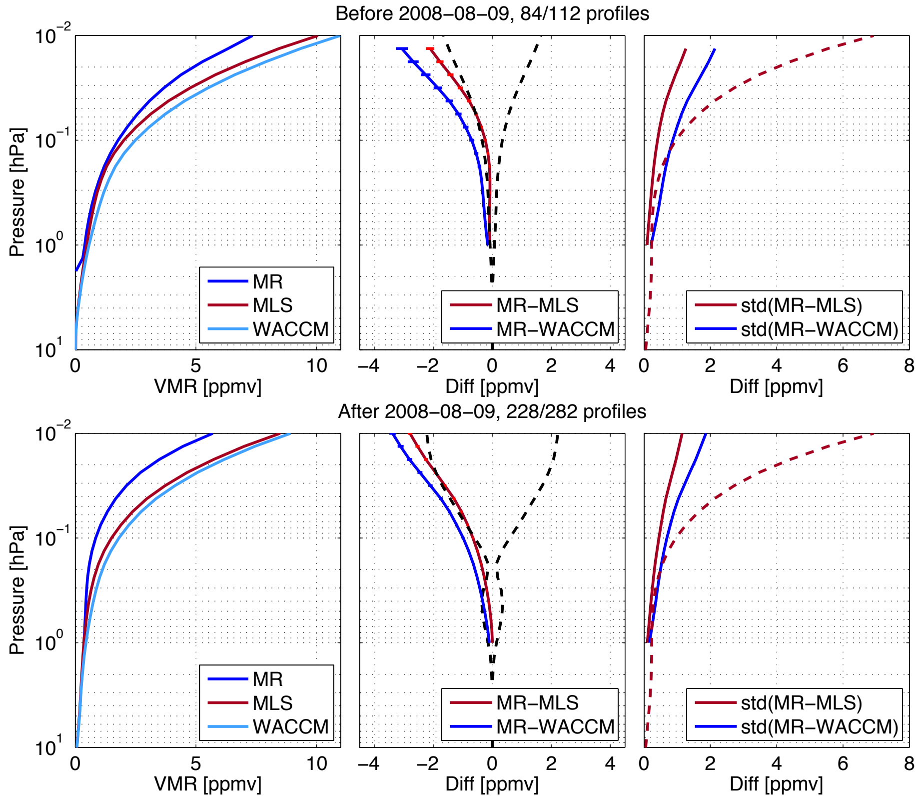

Fig. 8. Intercomparison between BAS microwave radiometer (MR) and MLS (red) or SD-WACCM (light blue), respectively. Left: mean coincident profiles of BAS radiometer (blue), MLS and SD-WACCM. Middle: bias with standard error and estimated systematic error of the BAS radiometer. Right: standard deviation of difference and combined random errors of MLS and the BAS radiometer (red dashed).

ESSDD
6, 1–26, 2013

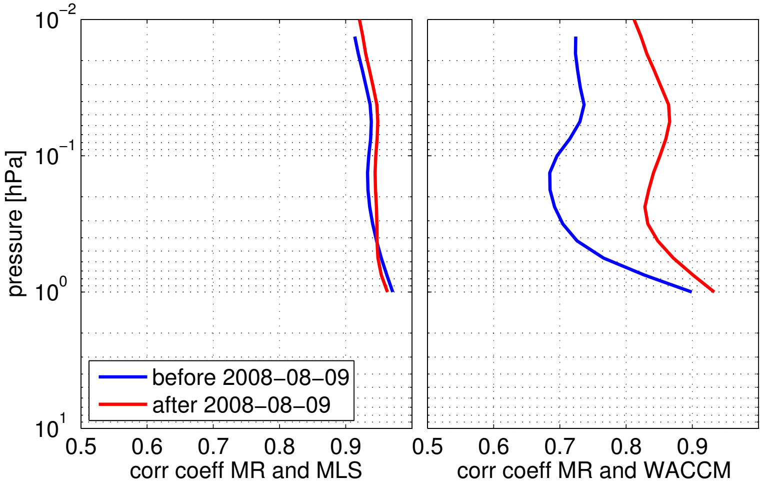

Fig. 9. Correlation coefficients between timeseries before (blue) and after (red) 9 August 2008. Left: BAS radiometer – MLS. Right: BAS radiometer – SD-WACCM.